waste

Article

Multifaceted Surface Analysis of Municipal Solid Waste Incineration Fly Ash by Water Repellent Treatment with Fatty Acid

Taiga Kaseda [1], Hibiki Shirata [1] and Yuya Koike [1,2,*]

[1] Applied Chemistry Course, Graduate School of Science and Technology, Meiji University, 1-1-1 Higashimita, Tama-ku, Kawasaki 214-8571, Kanagawa, Japan; tiger777@meiji.ac.jp (T.K.); ce234026@meiji.ac.jp (H.S.)
[2] Department of Applied Chemistry, School of Science and Technology, Meiji University, 1-1-1 Higashimita, Tama-ku, Kawasaki 214-8571, Kanagawa, Japan
* Correspondence: koi@meiji.ac.jp; Tel.: +81-44-934-7209

Abstract: In this study, we aimed to conduct a multifaceted surface analysis of water repellent-treated municipal solid waste incineration (MSWI) fly ash to determine the suppression mechanism of fatty acid elution. The surface of water repellent-treated MSWI fly ash was analyzed using scanning electron microscopy, Fourier-transform infrared spectroscopy, and X-ray diffraction analyses. Scanning electron microscopy revealed the absence of needle-shaped crystals but distinct particle agglomeration in the water repellent-treated fly ash. Fourier-transform infrared spectroscopy revealed that the water repellent treatment caused fatty acids to form esters with aluminosilicates in the MSWI fly ash. Crystalline phase analysis of the water repellent-treated fly ash before and after the leaching test via X-ray diffraction revealed the presence of fatty acids on the fly ash surface and retention of the fatty acid coating. Overall, the multifaceted surface analysis revealed that water repellent treatment suppressed heavy metal elution by covering the surface of MSWI fly ash with hydrophobic groups.

Keywords: multifaceted surface analysis; surface conditions; municipal solid waste incineration fly ash; fatty acids

Citation: Kaseda, T.; Shirata, H.; Koike, Y. Multifaceted Surface Analysis of Municipal Solid Waste Incineration Fly Ash by Water Repellent Treatment with Fatty Acid. *Waste* **2024**, *2*, 520–533. https://doi.org/10.3390/waste2040028

Academic Editors: Antonella Angelini and Carlo Pastore

Received: 25 October 2024
Revised: 29 November 2024
Accepted: 17 December 2024
Published: 19 December 2024

1. Introduction

Municipal solid waste incineration (MSWI) fly ash has more Pb and ^{137}Cs than the MSWI bottom ash [1]. Concentrated hazardous metals mainly exist as chlorides that are easily soluble in water [1]. Hazardous metals in MSWI fly ash are released into the environment via water [2–4]. Animals and plants in ecosystems concentrate toxic metals released into the environment. These substances can be hazardous to human health if absorbed [2–4]. Therefore, MSWI fly ash is required to be treated to prevent the leaching of hazardous metals when it is landfilled. Many studies have performed insolubilization treatment of hazardous metals in MSWI fly ash [5–8]. Cement and geopolymer solidification were focused on as effective insolubilization treatments. The reason is that the aluminosilicate contained in MSW fly ash has the same composition as the raw material for the solidification agent. Research has been conducted on the recycling of cement-solidified MSWI fly ash as building materials [9]. When MSW fly ash is solidified with cement, heavy metals are converted into hydroxides and carbonates inside the solidified body [9–12]. These compounds are insoluble in water and exist inside the cement-solidified body. It has been reported that insoluble heavy metals present in cement-solidified bodies are captured by cement hydrates [12]. The mechanism of elution suppression of heavy metal from MSWI fly ash by geopolymer solidification is different from that by cement solidification. Heavy metals in MSWI fly ash are encapsulated within the geopolymer solidification [13,14]. Heavy metals are immobilized as cations in the three-dimensional structure by aluminosilicates in the geopolymer [8]. However, geopolymer solidification of MSWI fly ash also increases its volume, as does cement solidification. This puts a strain on land for reclaiming MSWI fly ash. Therefore, insolubilization methods with little volume change are being considered. Representative treatment methods include washing with pure water [15], extraction with acidic liquids [16], and insolubilization treatment using dithiocarbamic acid chelating agents [17]. Washing with pure water or extraction with an acidic liquid requires concentrating hazardous metals from the extract [15,16]. Traditional washing methods require the treatment of wash water containing toxic compounds [15]. Dithiocarbamic acid chelating agents have metal selectivity for complex formation [17]. There is a need to propose an insolubilization method that is easy to operate and has an elution suppression effect for large amounts of metal elements. We focused on water repellent treatment to solve this problem. Water repellent treatment [18], an insolubilization method, is used to suppress the elution of hazardous metals from MSWI fly ash by modifying its surface with a water repellent. We previously reported that commercially available silane-based water repellents [19] and higher fatty acids, such as oleic acid [20,21], suppress the elution of metal elements from MSWI fly ash. Silane-based water repellents chemically modify the silanol groups of aluminosilicates contained in MSWI fly ash [19]. As a result, the silanol groups are converted to dimethylsiloxane groups. The methyl group in the dimethylsiloxane group has hydrophobic properties, which reduces contact with water [22]. Chemical modification using oleic acid is different from that of silane-based water repellents. It has been reported that the surface tension of MSWI fly ash is reduced by covering MSWI fly ash with oleic acid [19]. However, most studies have evaluated leaching characteristics only using the Japanese leaching test-13 (JLT-13) [23]. To the best of our knowledge, no analytical studies have assessed the surface conditions of MSWI fly ash after water repellent treatment to date. In addition, the mechanism by which water repellent treatment suppresses the elution of heavy metals present in MSWI fly ash is unclear. Therefore, multifaceted analysis of MSWI fly ash surfaces is necessary to elucidate the suppression mechanism of heavy metal elution by water repellent treatment.

Water repellent-treated materials are generally analyzed by observing the surface via scanning electron microscopy (SEM) [24,25] or mixing the material with water to assess the water repellent effect [26]. SEM can be used to investigate changes in surface conditions by observing materials before and after water repellent treatment. This result allows us to estimate the affinity between the water repellent and material based on the surface conditions of the water repellent-treated material [27]. Some studies have investigated water repellent-treated glass [24] and fibers [25,26]. In this study, we aimed to observe the surface of water repellent-treated MSWI fly ash using SEM, Fourier-transform infrared (FT/IR) spectroscopy, and X-ray diffraction (XRD) analyses. FT/IR can be used to qualitatively characterize the functional groups of organic and inorganic compounds by measuring the transmittance of infrared light [28]. Previous studies have analyzed water repellent treatments using FT/IR spectroscopy [29–32]. FT/IR spectroscopy can also be used to assess water repellent-treated MSWI fly ash. We analyzed MSWI fly ash before and after water repellent treatment by FT/IR. We thought that the obtained analytical results would enable us to investigate the functional groups related to the water repellent treatment. XRD can identify the crystalline and amorphous compounds in MSWI fly ash [33,34]. Ohbuchi et al. [34] identified the crystalline phase of MSWI fly ash and quantified it by Rietveld analysis. The results suggest that heavy metals in MSWI fly ash exist in an amorphous state [34]. However, there have been no reports on the measurement of the crystalline phase in water repellent-treated MSWI fly ash by XRD; therefore, it was used to assess the chemical reactions between fatty acids and metal compounds in this study.

In this study, the surface of water repellent-treated MSWI fly ash was investigated via SEM, FTIR spectroscopy, and XRD analyses. The surface conditions of MSWI fly ash after water repellent treatment were evaluated via multifaceted analysis using these three different analytical methods. Additionally, the suppression mechanism of heavy metal elution by fatty acids was explored by assessing the surface conditions of water repellent-treated MSWI fly ash.

2. Materials and Methods

2.1. MSWI Fly Ash and Water Repellent Treatment

MSWI fly ash was collected from a general waste incineration facility in the Kanagawa Prefecture, Japan, in 2021 (Figure 1).

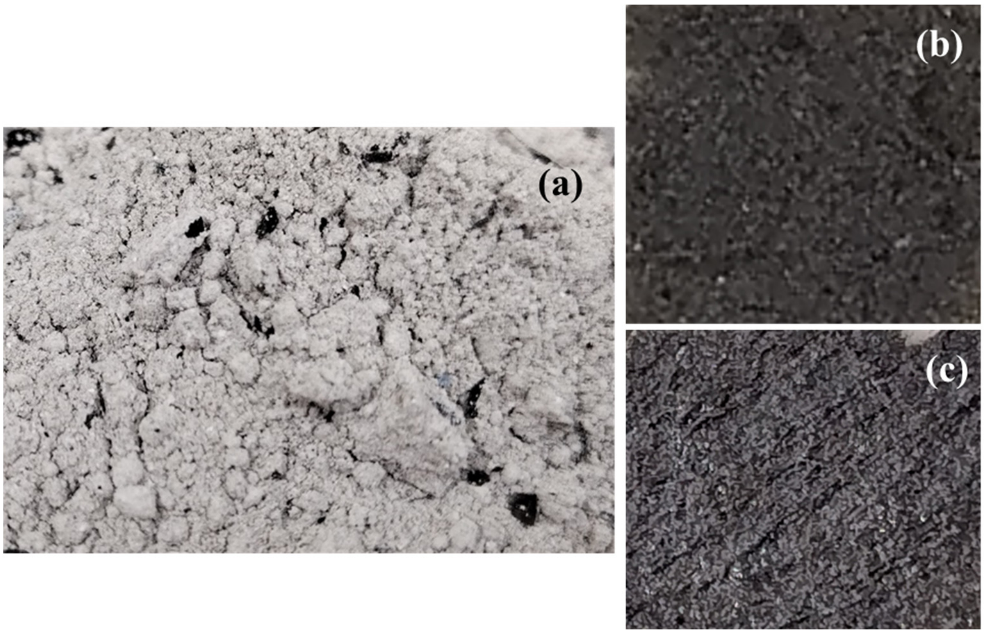

Figure 1. Photos of municipal solid waste incineration (MSWI) fly ash sampled at a municipal waste incinerator in Kanagawa prefecture (**a**), photos of OA (**b**) and IS (**c**).

MSWI fly ash is mainly generated by the incineration of food waste and paper and is not sprayed with slaked lime to inhibit the generation of dioxins [21]. General municipal solid waste is incinerated at a temperature of 800–1000 °C in a stoker-type incinerator. This is the temperature range in which dioxins are less likely to be produced when municipal solid waste (MSW) is incinerated [35]. The MSWI fly ash was ground in a ball mill (PULVERISETTE 6, Fritsch Japan, Kanagawa, Japan) at 300 rpm for 10 min to a uniform particle size and was used as raw fly ash (**RFA**). **RFA** was mixed with oleic acid or isostearic acid. Then, MSWI fly ash was mixed with two water repellents in a mass ratio of 1:1 (solid waste/water repellent). The mixed samples were dried at 20 °C for 1 h. Oleic acid (FUJIFILM Wako Pure Chemical Corporation, Osaka, Japan) and isostearic acid (FUJIFILM Wako Pure Chemical Corporation, Osaka, Japan; Figure 2), which exhibited a high elution suppression effect in a previous study by Akino et al. [21], were used as water repellents. Both fatty acids are monocarboxylic acids containing 18 carbon atoms. Moreover, they exist as liquids at room temperature and are easily mixed with MSWI fly ash.

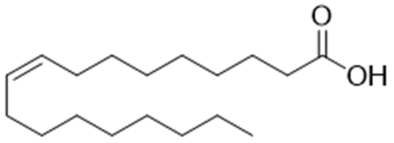

Oleic acid (**1**)

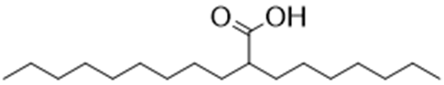

Isostearic acid (**2**)

Figure 2. Structures of oleic acid (**1**) and isostearic acid (**2**) used as water repellents.

RFA treated with oleic acid and isostearic acid as water repellents are hereafter denoted as **OA** and **IS**, respectively.

2.2. Apparatus

JLT-13 eluate was analyzed via inductively coupled plasma–atomic emission spectrometry (ICP-AES; Thermo Fisher Scientific, Waltham, MA, USA). ICP-AES conditions were set as follows: radio frequency power of 1150 W, coolant Ar flow of 12 L min^{-1}, auxiliary Ar flow of 0.5 L min^{-1}, nebulizer Ar flow of 0.5 L min^{-1}, substituted flow quantity of 100 rpm, and flow rate of 50 rpm. Next, concentrations of blank and the Cr, Fe, Cu, Cd, and Pb series were prepared to 0.1 mol L^{-1} using 1000 mg L^{-1} elemental standards (FUJIFILM Wako Pure Chemical Corporation, Osaka, Japan) and HNO_3 for the calibration of ICP-AES. ICP-AES emission wavelengths of 283.563 nm (Cr), 259.940 nm (Fe), 324.754 nm (Cu), 228.802 nm (Cd), and 220.353 nm (Pb) were used to assess these elements. In Japan, there are criteria for determining specific controlled industrial waste established by the Ministry of the Environment. Of hazardous metals investigated in this study, there are standards for Pb, Cr, and Cd: Pb: 0.3 mg/L; Cr: 1.5 mg/L; and Cd: 0.3 mg/L [36].

The surface properties of water repellent-treated MSWI fly ash were analyzed using SEM (JSM-6390LA; JEOL, Tokyo, Japan). The accelerating voltage of the device was set to 5.0 keV to suppress discharge due to electrolysis. FT/IR spectra of RFA, OA, and IS were measured via FT/IR spectroscopy (FT/IR 4000; JASCO, Tokyo, Japan) using the KBr tablet method. The wavenumber was set to 600 to 4000 cm^{-1}, and the absorbance was calculated from the obtained transmittance. The absorbance was calculated from the transmittance at 3359 cm^{-1}, 1708 cm^{-1}, and 1538 cm^{-1} using the following Equation (1):

$$\text{A} = 2 - log_{10}(\%T) \tag{1}$$

Then, crystalline phases of **RFA**, **OA**, and **IS** were qualitatively analyzed using XRD (MiniFlex 600; Rigaku Co., Tokyo, Japan). The XRD system was equipped with an X-ray tube with a Cu target (operated at 40 kV and 15 mA). The Bragg–Brentano focusing optical system was used for analysis. The intensity of each peak was recorded from 5° to $70°/2\theta$ in steps of 0.01°, with a scanning speed of 1° min^{-1}. Phase identification was performed using integrated X-ray powder diffraction software (SmartLab Studio II; Rigaku Co. Tokyo, Japan).

2.3. JLT-13

JLT-13 is among the most rapid and easy methods to assess the leachability of heavy metals from various types of waste in a waste landfill [37]. For JLT-13, a mixture of pure water and classified MSWI fly ash (S/L = 0.1) was subjected to continuous shaking for 6 h at room temperature. A mechanical shaker (TBK 602DA; Advantec Inc., Tokyo, Japan) was used to prepare the eluted solutions from fly ash. The velocity of the shaker was approximately 200 rpm. After shaking, the eluted solutions were separated from the corresponding MSWI fly ash using a filter paper (Whatman glass microfiber filters; 100 mmφ; GE Healthcare Life Science Japan, Tokyo, Japan).

3. Results and Discussion

3.1. Suppression of Heavy Metal Elution by Water Repellent Treatment

Here, suppression of heavy metal elution by water repellent treatment of MSWI fly ash was investigated. The elution suppression effect of water repellent treatment with two types of fatty acids (oleic and isostearic acids) was evaluated using JLT-13. Concentrations of Cr, Fe, Cu, Cd, and Pb in the OA and IS eluates are shown in Figure 3. Typical MSWI fly ash particles are finer than 500 μm in size [37]. MSWI fly ash is not crushed during intermediate processing. It was milled to perform the analysis, but also treated with fatty acids without ball-milling for application in the intermediate treatment. Water repellent treatment is possible by coating the surface of MSWI fly ash with fatty acid without crushing (Figure 3). Water repellent treatment using fatty acid provides hydrophobicity to the surface of MSWI fly ash without relying on crushing. We would like to study the durability due to mechanical stress further, as this is important information for landfill disposal.

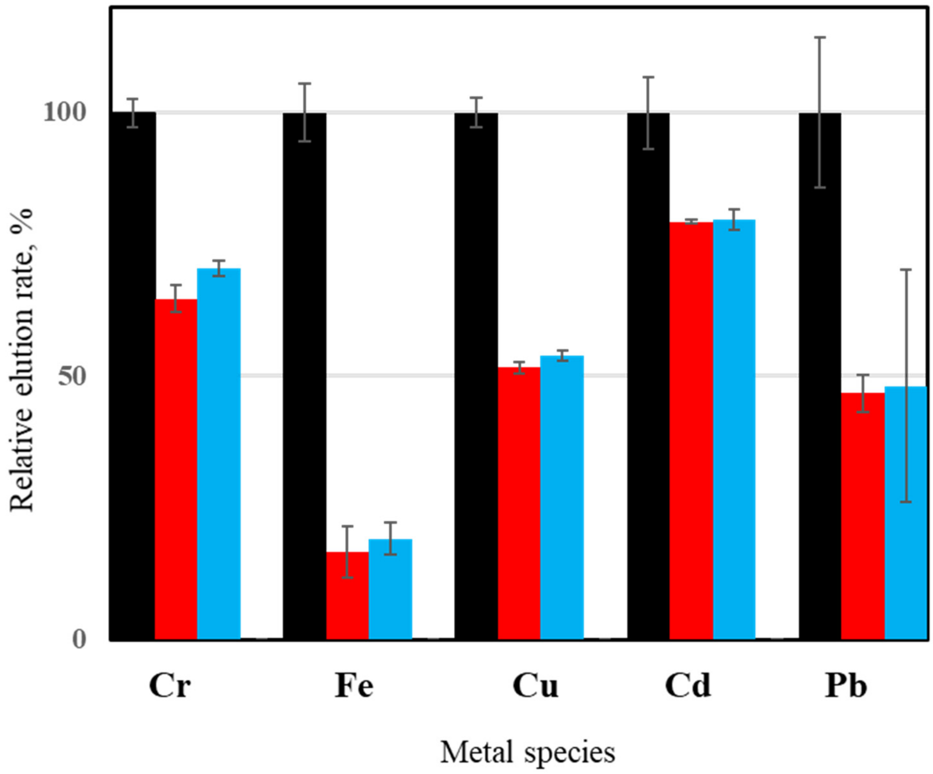

Figure 3. Relative elution rate * of heavy metals from MSWI fly ash treated with oleic acid (🟥) and isostearic acid (🟦) by JLT-13. * Elution rate normalized with the elution rate of raw MSWI fly ash as 100% (■).

The relative elution rate of each heavy metal was calculated by normalizing the heavy metal elution rate with that of **RFA** as 100%. These results indicate that mixing fatty acids with MSWI ash has a high elution suppression effect on Fe, one of the heavy metal elements contained in MSWI fly ash. Fe is not easily concentrated in MSWI fly ash and is an element that does not dissolve much from MSWI fly ash [38]. Water repellent treatment using fatty acids reduced the elution of Cu and Pb into water by about half. Takaoka et al. [39] reported that Cu is a compound in which $CuCl_2$ and CuO are easily dissolved in water. We believe that the water repellent treatment of MSWI fly ash prevented these compounds from contacting water, thereby reducing heavy metal leaching into the water. In particular, Cu and Pb are designated as specific hazardous metals worldwide. Regarding Cu in MSWI fly ash, the amount of Cu eluted increases as $Cu(OH)_2$ increases during the process of generating MSWI fly ash [40]. Among the Pb present in MSWI fly ash, $PbCl_2$ and PbO are easily soluble in water. Regarding Pb, it has been reported that Pb present in MSWI fly ash is dissolved in the form of $PbCO_3$ and $Pb(OH)_2$ under strongly alkaline conditions [41]. The background to these problems is that hydrated lime is sprayed onto MSWI fly ash from MSW incineration, but other causes are being investigated. Similar results were obtained in reports by Ogawa et al. [18] and Akino et al. [21]. We compared the elution suppression effect of water repellent treatment with that of solidification treatment (Table 1).

In Japan, cement solidification is used to suppress the elution of heavy metals from MSWI fly ash. It was reported that the elution of heavy metals from cement-solidified MSWI fly ash was suppressed by 40–50% [10]. Therefore, similar results were obtained without physically solidifying the MSWI fly ash. Water repellent treatment using fatty acids is effective in suppressing the elution of Fe, Cr, and Pb contained in MSWI fly ash. On the other hand, the water repellent treatment with fatty acids had little effect on suppressing the elution of Cr and Cd in MSWI fly ash. Cr contained in MSWI fly ash exists not only in the form of chlorides, but also in the form of oxides, hydroxides, carbonates, and complexes [42]. Cr hydroxide and Cr carbonate are easily dissolved under acidic conditions [43]. Therefore, we believe that mixing fatty acids with MSWI fly ash promoted the dissolution of Cr in the form of hydroxide and carbonate. Cd contained in MSWI fly ash exists mainly as chloride and hydroxide. There have been many reports that hydroxides are eluted under strong alkaline conditions [40,43]. Funatsuki et al. [44] reported that small amounts of $Cd(OH)_2$ were present in the eluate from MSWI fly ash. In this study, we could not identify $Cd(OH)_2$ in the leaching solutions of **OA** and **IS**. Takaoka et al. [39] also suggested that the proportion of $Cd(OH)_2$ increases with changes in pH in m MSWI fly ash. Based on the above, we are investigating the chemical forms and leaching behavior of Cr and Cd in water repellent-treated MSWI fly ash in order to suppress the leaching of Cr and Cd. Moreover, Akino et al. [21] reported that **OA** produces coagulant substances during JLT-13 that inhibit its elution suppression effect. However, this phenomenon was not observed in this study. Therefore, further investigation is necessary to assess the formation of the solidified material.

Table 1. Comparison of heavy metal leaching control treatment methods for MSWI fly ash.

Treatment	Elution Suppression Effect	Advantage	Disadvantage
Water repellent	**16–19% (Fe)** **45–55% (Pb, Cu)**	**Easy processing operations** **No increase in volume**	**Difficult tocontrol Cr and Cd elution**
Cement solidication [10,11]	**Not detected (Fe)** **40–50% (Pb, Cd)**	**Easy processing operations** **Low cost**	**Increase in volume** **Metal elution by cracks**
Geopolymer solidication [12,13]	**Not detected (Fe)** **40–94% (Pb, Cd)**	**Easy processing operations** **No CO_2 emissions**	**Increase in volume** **Weak to acidity**
Chelating agent stabilization [15]	**41% (Fe)** **27–45% (Pb, Cd)**	**Easy processing operations** **Low cost**	**Dependence on the Cl content in MSWI fly ash**

3.2. SEM Images of RFA, OA, and IS

Figure 4 shows the SEM images of MSWI fly ash before and after water repellent treatment using oleic and isostearic acids.

Before the water repellent treatment, a substance with many voids was observed on the surface of MSWI fly ash [45]. MSWI fly ash is produced by rapid cooling during the process of MSWI followed by collection in a dust collector [46]. As a result, the substances contained in MSW tend to be amorphous. MSWI fly ash also consists of chlorides such as NaCl and KCl, and ash from paper, rubber, and plastic [47]. The latter has more voids due to loss of moisture during incineration [48]. On the other hand, in the SEM images of the water repellent-treated MSWI fly ash using fatty acids, no irregularities were observed on the surface of the water repellent-treated MSWI fly ash using oleic acid (Figure 4c) and isostearic acid (Figure 4e). Liu et al. [49] reported that water repellent treatment causes MSWI fly ash particles to agglomerate with a rough surface. In this study, SEM images showed that the surface shape of MSWI fly ash changed after water repellent treatment due to the penetration of fatty acids. Roughening the surface reduces the surface tension of water [22]. A water repellent layer was also observed on the MSWI fly ash surface, consistent with previous reports [18,19]. Ogawa et al. [18] reported that by applying a water repellent treatment to MSWI fly ash, fatty acids penetrate into the pores of the MSWI fly ash and form a water repellent layer. In addition, the volume increase rate of the MSWI fly ash that has been treated for water repellency is less than 1% [18]. This volume increase rate is much smaller than that of solidification treatments such as cement and geopolymers. The SEM observations suggest that MSWI fly ash can be made water repellent simply by mixing it with fatty acids. Furthermore, the water repellent-treated MSWI fly ash is more compact than the solidified MSWI fly ash.

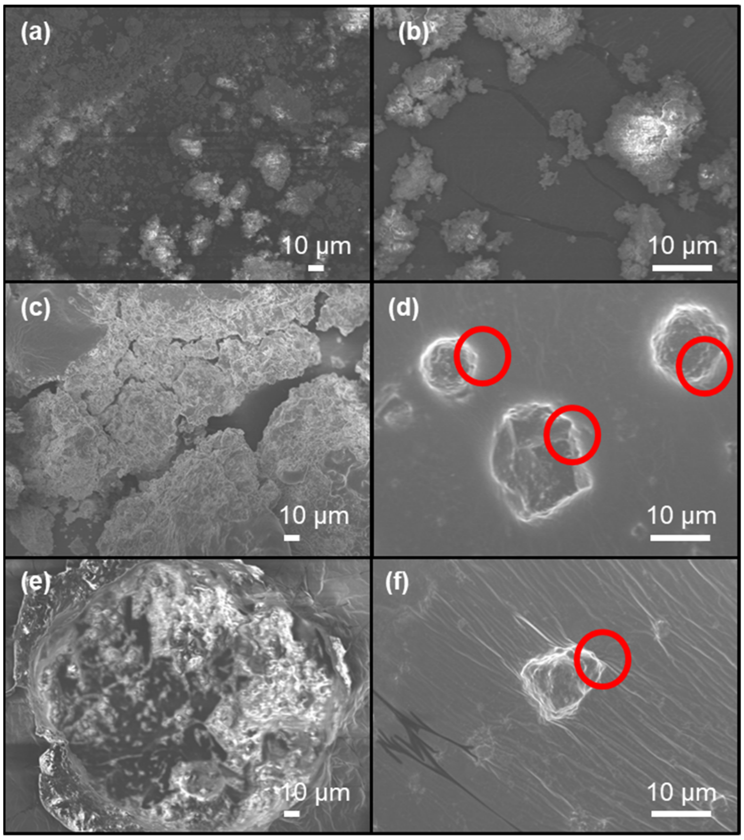

Figure 4. SEM images of MSWI fly ash (**a**,**b**) by water repellent treatment with oleic acid (**c**,**d**) and isostearic acid (**e**,**f**). Red Circles: water repellent layer.

3.3. Qualitative Analysis of Water Repellent-Treated RFA via FTIR Spectroscopy

FT/IR spectra of **RFA** (**a**), oleic acid (b), **OA** (**c**), isostearic acid (**d**), and IS (**e**) measured using the KBr tablet method are shown in Figure 5.

The O–H and Si–O stretching vibrations of **RFA** in Figure 5a were 3359, 1643, and 1095 cm^{-1}, respectively. These stretching vibration peaks originate from silicates. Harja et al. [50] and Katara et al. [51] identified the wavenumbers originating from aluminosilicates in **RFA**. From Figure 4b,d, the peak at 2924 cm^{-1} of the fatty acid-derived peaks indicates the C-H asymmetric stretching vibration in the long-chain alkyl group. The peaks representing the C=O stretching vibration are 1709 cm^{-1} for oleic acid (**b**) and 1701 cm^{-1} for isostearic acid (**d**) [52]. Considering the peak at 3359 cm^{-1} (**A**) in Figure 5a,c,e, the absorbance due to the O-H stretching vibration of aluminosilicates in **RFA** was 3.17. The absorbance calculated from the peak (**A**) decreased to 0.17 and 0.22 for OA and IS, respectively. In Figure 5b,d, no peaks at around 3400 cm^{-1} indicating O-H stretching vibrations were observed in the spectra of oleic acid and isostearic acid. The reason for this is that fatty acid molecules self-associate through hydrogen bonds between the carboxyl groups to form dimers [52]. As a result, the hydrocarbon groups cover the carboxyl groups, making it difficult to observe the O-H stretching vibration. In the FT/IR spectra of the water repellent-treated MSWI fly ash, the peak at 1708 cm^{-1} (**B**) decreased from 1.03 to 0.02, the peak at around 1538 cm^{-1} increased from 0.02 to 0.13, and the peak at around 1467 cm^{-1} decreased from 0.28 to 0.13 (**C** and **D**). When fatty acids form dimers, a sharp peak at around 1710 cm^{-1} indicating the C=O stretching vibration is observed, but no peak at around 1538 cm^{-1} is observed. It has been reported that when fatty acids change from dimers to monomers, a peak at around 1538 cm^{-1} indicating the asymmetric stretching vibration of C=O and a peak at around 1467 cm^{-1} indicating the symmetric stretching vibration are observed to the same extent. It has been reported that when fatty acids change from dimers to monomers [52], the FT/IR spectrum shows a peak at around 1557 cm^{-1}

indicating the asymmetric stretching vibration of C=O and a peak at around 1428 cm^{-1} indicating the symmetric stretching vibration of the fatty acid ion [31]. Therefore, it is presumed that the fatty acids mixed with MSWI fly ash are converted from dimers to monomers. In addition, peaks were observed at 1634 cm^{-1} for **OA** and 1687 cm^{-1} for **IS**. These peaks indicate the C=O stretching vibration in the ester bond. The above results suggest that the carboxyl and hydroxyl groups of the fatty acids at the ends of the aluminosilicates in MSWI fly ash form ester bonds [31]. Because the hydroxyl groups have been converted to ester groups, MSWI fly ash has a lower affinity for water. Similar results have been reported by Liu et al. [49] and Sakthivel et al. [53]. Therefore, when MSWI fly ash is mixed with a water repellent, the hydrophilic carboxyl group modifies the hydroxyl group at the end of the aluminosilicates [49]. As a result, the hydroxyl groups are converted to long-chain alkyl groups, which cover the surface of the MSWI fly ash, making the MSWI fly ash hydrophobic.

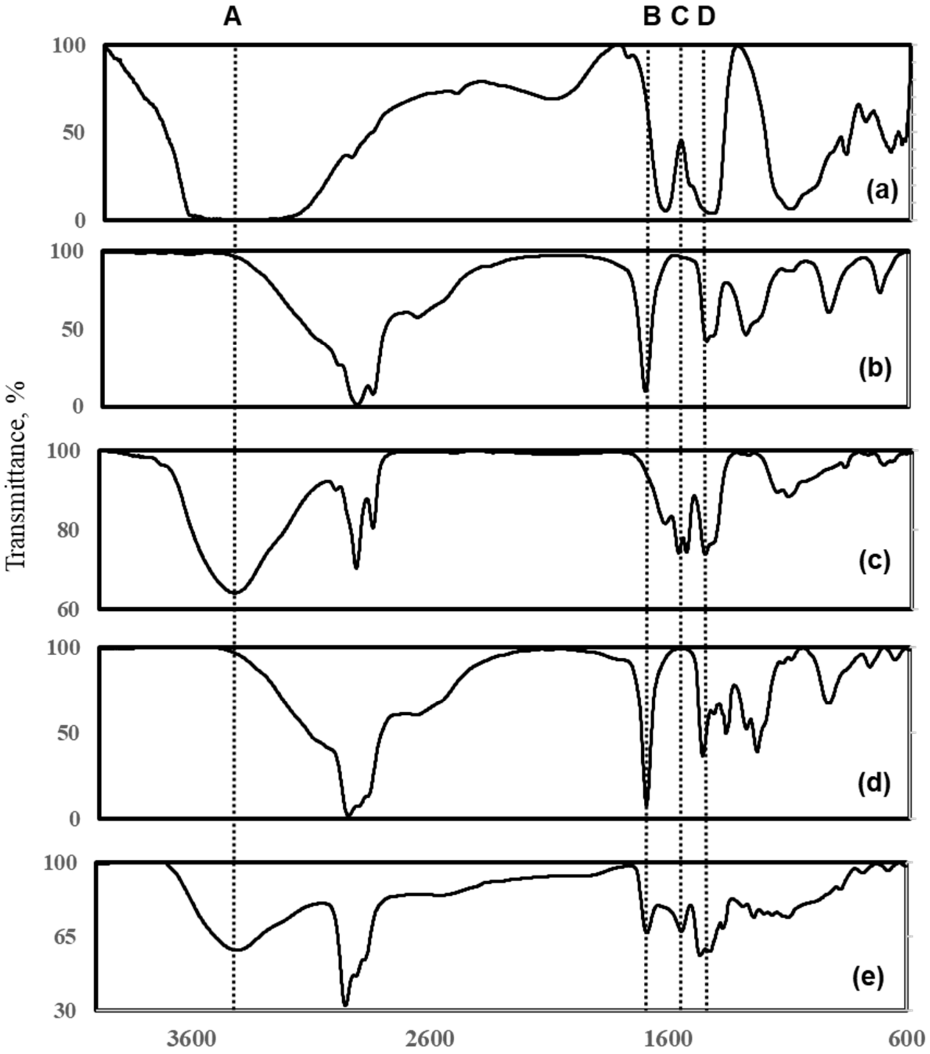

Figure 5. FT/IR spectra of MSWI fly ash (**a**), oleic acid (**b**), oleic acid-treated fly ash (**c**), isostearic acid (**d**), isostearic acid-treated fly ash (**e**). Dot lines are characteristic wavenumbers originating from fatty acids. Dot Line A: 3359 cm^{-1}; B: 1709 cm^{-1}; C: 1538 cm^{-1}; D: 1467 cm^{-1}.

3.4. Crystal Phase Analysis via XRD

XRD patterns of **RFA** before and after water repellent treatment are shown in Figure 6. Table 2 shows the crystalline phase in MSWI fly ash and water repellent-treated samples observed before and after JLT-13.

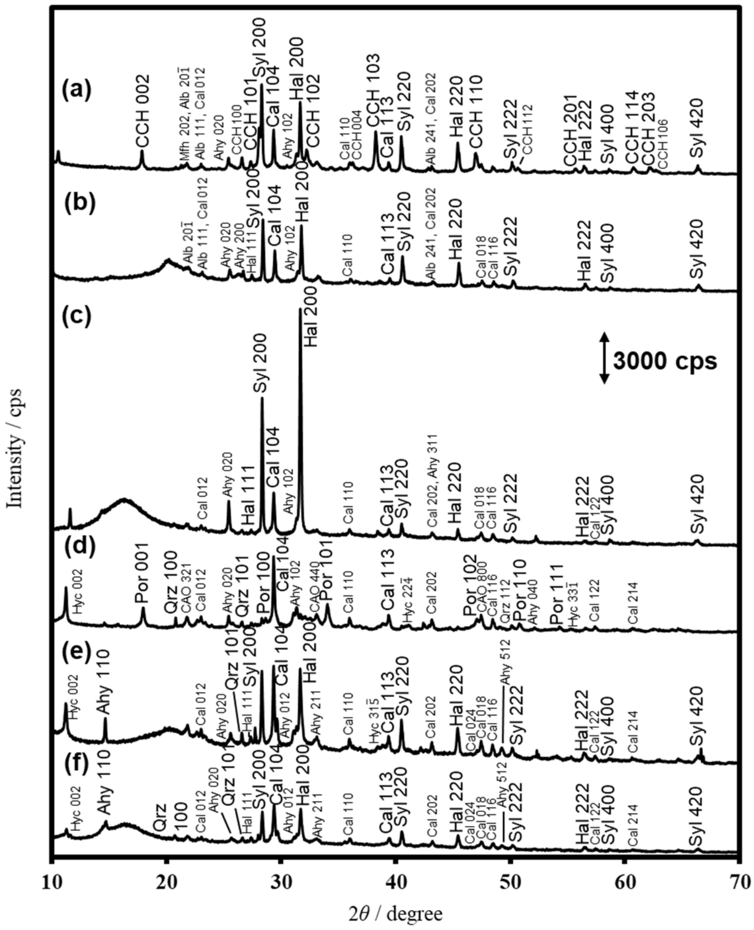

Figure 6. X-ray diffraction (XRD) images of MSWI fly ash with and without water repellent treatment before and after JLT-13. (**a**) MSWI fly ash before JLT-13, (**b**) **OA** before JLT-13, (**c**) **IS** before JLT-13, (**d**) MSWI fly ash residue from JLT-13, (**e**) **OA** residue from JLT-13, (**f**) **IS** residue from JLT-13. Hal: halite (NaCl); CCH: calcium chloride hydroxide (CaCvvlOH); Syl: sylvite (KCl); Alb: albite ($NaAlSi_3O_8$); Cor: cordierite ($Mg_2Al_3(AlSi_5O_{18})$); Qrz: quartz (SiO_2); Cal: calcite ($CaCO_3$); Geh: gehlenite ($Ca_2Al_2SiO_7$); Ahy: anhydrite ($CaSO_4$); Bas: bassanite ($CaSO_4(H_2O)_{0.5}$); Tob: tobermorite ($Ca_4(Si_6O_{15})(OH)_2(H_2O)_5$); Por: portlandite ($Ca(OH)_2$); CAO: calcium aluminum oxide ($Ca_3Al_2O_6$); Hyc: hydrocalumite ($Ca_2Al(CO_3)_{0.25}Cl_{0.5}(OH)_6(H_2O)_{2.4}$); Mfh: magnesio-ferri-hornblende ($Ca_2(Mg_4Fe^{3+})[(Si_7Al)O_{22}](OH)_2$).

Table 2. The crystalline phase in MSWI fly ash (**RFA**) and water repellent-treated samples (**OA** and **IS**) observed before and after JLT-13.

	Before JLT-13			**After JLT-13**		
	RFA	**OA**	**IS**	**RFA**	**OA**	**IS**
Halite	✓	✓	✓	-	✓	✓
Sylvite	✓	✓	✓	-	✓	✓
Anhydrite	✓	✓	✓	✓	✓	✓
Calcite	✓	✓	✓	✓	✓	✓
Calcium aluminum oxide	-	-	-	✓	-	-
Calcium Chloride Hydroxide	✓	-	-	-	-	-
Hydrocalumite	-	-	-	✓	✓	✓
Portlandite	-	-	-	✓	-	-
Albite	✓	✓		-	-	-
Quartz	-	-	-	✓	✓	✓

Halite (NaCl), sylvite (KCl), calcium chloride hydroxide (CaClOH), calcite ($CaCO_3$), portlandite ($Ca(OH)_2$), and anhydrite ($CaSO_4$) were identified in the XRD pattern of **RFA** (Figure 6a). Chlorides, carbonates, and sulfates are typical crystalline phases in **RFA** [33,45]. Aluminosilicates [33,34] were also identified as **RFA**. XRD patterns of **OA** (Figure 6b) and **IS** (Figure 6c) showed the presence of halite (NaCl) and sylvite (KCl), which are easily soluble in water [1,33,54]. Furthermore, crystalline phase analysis revealed haloes originating from the fatty acids coating the fly ash surface in the diffraction patterns of **OA** and **IS**. A halo peak (**OA**: approximately 19°; **IS**: approximately 16°) was detected at a similar diffraction angle in the XRD patterns of both fatty acids used as water repellents. In contrast, peaks corresponding to calcium chloride hydroxide and portlandite disappeared from MSWI fly ash patterns after water repellent treatment. Furthermore, there was no change in the diffraction intensity in the crystalline phase identified from the XRD pattern after the water repellent treatment using fatty acids. Omote et al. [55] reported that when measuring the intensity of liquid organic matter by XRD, a halo peak is observed at approximately 20°. Calcium fatty acids can be formed by the chemical reactions of calcium salts [20]. In the future, we plan to qualify calcium fatty acids using FT/IR and XRD, and investigate the detailed chemical reactions involved in water repellent treatment using fatty acids. Halite (NaCl) and sylvite (KCl) were not identified in the XRD pattern of **RFA** after JLT-13 in Figure 6d. The presence of water-soluble compounds in the leaching test residue indicated that the water repellent-treated MSWI fly ash was hydrophobic (Figure 6e,f). Halo peaks of **OA** and **IS** before and after JLT-13 treatment revealed that the fatty acid coating was retained after the leaching test. Furthermore, crystalline phase analysis before and after the leaching test confirmed that the fatty acid coating was retained in water repellent-treated MSWI fly ash. It is inferred that the water repellent treatment of MSWI fly ash using fatty acids is not destroyed under strong shaking conditions in pure water. From these results, it can be said that no chemical reaction was confirmed between fatty acids and alkali metal compounds even after the water repellent treatment of MSWI fly ash. We have confirmed through leaching tests using JLT-13 that heavy metals are leached from water repellent-treated MSWI fly ash. These results suggest that it is necessary to consider methods for quantifying crystalline phases such as halite (NaCl) and sylvite (KCl). Since there is a possibility that a chemical reaction occurred between fatty acids and calcium compounds, a detailed investigation is required. We will focus on the chemical form and content of Ca in MSWI fly ash, rather than on the addition of $Ca(OH)_2$.

4. Conclusions

In this study, MSWI fly ash samples treated with oleic acid and isostearic acid (OA and IS, respectively), which effectively suppressed heavy metal elution in a previous study, were used in this study. Both oleic acid and isostearic acid have 18 carbons in their structures. However, oleic acid, a linear long-chain fatty acid, and isostearic acid, a branched-structure fatty acid, have different molecular structures. The purpose of this study is to clarify the elution suppression mechanism of hazardous metals in MSWI fly ash. It also aims to consider the relationship between the molecular structure of fatty acids and the elution suppression mechanism. The results of the elution test using JLT-13 showed that oleic acid and isostearic acid were effective in suppressing the elution of Fe, Cu, and Pb. Water repellent treatment decreased the leaching quantity from MSWI fly ash from 1.86 ppm to 0.30 ppm for Fe, from 5.13 ppm to 2.65 ppm for Cu, and from 2.11 ppm to 1.00 ppm for Pb. These results indicate that the water repellent treatment had the same effect of suppressing elution as the cement solidification treatment. It is thought that if the number of hydrocarbons in the fatty acids is the same, the elution suppression effect will tend to be similar. The surface of water repellent-treated MSWI fly ash was subjected to multifaceted analysis using three analytical methods: SEM, FT/IR spectroscopy, and XRD. SEM revealed particle agglomeration and the presence of a water repellent layer in the water repellent-treated MSWI fly ash. FT/IR spectroscopy revealed that the carboxyl group derived from the water repellent and hydroxyl group at the end of the aluminosilicate salt formed an ester bond. XRD, which was used to identify the crystalline phase, showed that water repellent treatment retained the fatty acid repellent layer and inhibited the elution of highly water-soluble metal compounds. Multifaceted surface analysis was used to estimate the changes in the surface conditions of MSWI fly ash after water repellent treatment. Water repellent treatment caused the carboxyl groups of fatty acids to bond with the hydroxyl groups of aluminosilicates in MSWI fly ash via electrostatic interactions. Consequently, hydrocarbon groups were introduced at the ends of the aluminosilicates. The surface of MSWI fly ash was hydrophobic and prevented contact with water, thereby suppressing the elution of heavy metals (Figure 7). Notably, no chemical reactions occurred between the fatty acids and alkaline metal compounds on the MSWI fly ash surface. Leaching tests of MSWI fly ash revealed intact ester bonds between the fatty acids and aluminosilicates after water repellent treatment. Therefore, MSWI fly ash mixed with fatty acids has water repellency due to the hydrophobic groups covering its surface. Multifaceted surfaced analysis of water repellent-treated MSWI fly ash will contribute to the elucidation of the suppression mechanism of hazardous metals elution by water repellent treatment. Furthermore, the volume increase of the water repellent treatment is smaller than that of the solidification treatment. The water repellent treatment is expected to be a stabilization method for larger quantities of MSWI fly ash.

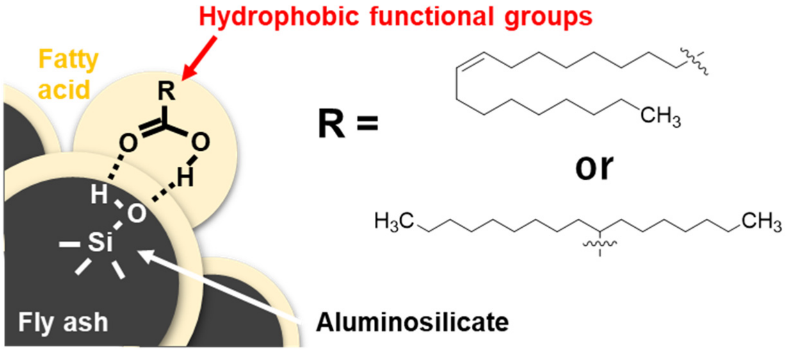

Figure 7. A schematic diagram of the estimated elution suppression mechanism by water repellent treatment of MSWI fly ash.

Author Contributions: Conceptualization, Y.K.; methodology, Y.K. and T.K.; validation, T.K. and H.S.; formal analysis, Y.K. and T.K.; investigation, T.K., H.S. and Y.K.; data curation, T.K. and H.S.; writing—original draft preparation, T.K.; writing—review and editing, T.K. and Y.K.; supervision, Y.K.; project administration, Y.K. All authors have read and agreed to the published version of the manuscript.

Funding: This research received no external funding.

Institutional Review Board Statement: Not applicable.

Informed Consent Statement: Not applicable.

Data Availability Statement: No new data were created or analyzed in this study. Data sharing is not applicable to this article.

Acknowledgments: The authors would like to thank everyone involved at the general waste incineration facility in Kanagawa Prefecture for providing us with urban waste incineration fly ash. Special thanks are due to the Meiji University Center for Collaborative Innovation and Incubation for their support and help in the SEM observation. We would like to thank Narihito Ogawa and Takayuki Honda at Meiji University, for their continued guidance and encouragement throughout this work. We are grateful to the members of the Radiochemistry Laboratory at Meiji University for their cooperation.

Conflicts of Interest: The authors declare no conflicts of interest.

References

1. Koike, Y.; Fujii, K.; Saito, R.; Ogawa, N.; Ohbuchi, A. Chemical state analysis of heavy metals and radioactive cesium in municipal solid waste incineration fly ash contaminated with radioactive cesium released by the FDNPP accident. *Anal. Sci.* **2021**, *37*, 1565–1570. [CrossRef] [PubMed]
2. Tian, Q.; Guo, B.; Nakama, S.; Sasaki, K. Distributions and Leaching Behaviors of Toxic Elements in Fly Ash. *ACS Omega* **2018**, *3*, 13055–13064. [CrossRef] [PubMed]
3. Parajuli, D.; Tanaka, H.; Hakuta, Y.; Minami, K.; Fukuda, S.; Umeoka, K.; Kamimura, R.; Hayashi, Y.; Ouchi, M.; Kawamoto, T. Dealing with the Aftermath of Fukushima Daiichi Nuclear Accident: Decontamination of Radioactive Cesium Enriched Ash. *Environ. Sci. Technol.* **2013**, *47*, 3800–3806. [CrossRef]
4. Kido, G.; Takasaki, M.; Minami, K.; Tanaka, H.; Ogawa, H.; Kawamoto, T.; Yoshino, K. Analysis of Cs-adsorption behavior using a column filled with microcapsule beads of potassium copper hexacyanoferrate. *J. Nucl. Sci. Technol.* **2017**, *54*, 1157–1162. [CrossRef]
5. Kakehi, J.-I.; Kamio, E.; Takagi, R.; Matsuyama, H. Effects of Coexistent Ions on $^{137}Cs^+$ Rejection of a Polyamide Reverse Osmosis Membrane in the Decontamination of Wastewater with Low Cesium-137 Concentration. *Ind. Eng. Chem. Res.* **2017**, *56*, 6864–6868. [CrossRef]
6. Kobayashi, T.; Ohshiro, M.; Nakamoto, K.; Uchida, S. Decontamination of Extra-Diluted Radioactive Cesium in Fukushima Water Using Zeolite–Polymer Composite Fibers. *Ind. Eng. Chem. Res.* **2016**, *55*, 6996–7002. [CrossRef]
7. Qiu, Q.; Jiang, X.; Chen, Z.; Lu, S.; Ni, M. Microwave-Assisted Hydrothermal Treatment with Soluble Phosphate Added for Heavy Metals Solidification in MSWI Fly Ash. *Energy Fuels* **2017**, *31*, 5222–5232. [CrossRef]
8. Saito, R.; Kaseda, T.; Tasaki, R.; Matsuda, W.; Ohbuchi, A.; Ogawa, N.; Koike, Y. Insolubilization of Radioactive Cesium in Municipal Solid Waste Incineration Fly Ash by Geopolymer Solidification using Akadama Soil. *J. Jpn. Soc. Mater. Cycles Waste Manag.* **2022**, *33*, 18–29. [CrossRef]
9. Uehara, M.; Isogaya, S.; Yamazaki, A. Ion-exchange properties of hardened geopolymer paste prepared from fly ash. *Clay Sci.* **2009**, *14*, 127–133. [CrossRef]
10. Dote, Y.; Maruyama, T. Dissolution of Heavy Metals from Ground Materials Solidified with Portland Cement. *J. Jpn. Soc. Waste Manag. Expert.* **1998**, *9*, 188–197. [CrossRef]
11. Shimaoka, T.; Hanashima, M. The Behavior of Fly Ash Stabilized by Cement Solidification in Landfills. *Haikibutsugakkaishi* **1994**, *5*, 32–45. [CrossRef]
12. Tian, X.; Rao, F.; Morales-Estrella, R.; Song, S. Effects of Aluminum Dosage on Gel Formation and Heavy Metal Immobilization in Alkali-Activated Municipal Solid Waste Incineration Fly Ash. *Energy Fuels* **2020**, *34*, 4727–4733. [CrossRef]
13. Ren, X.; Wang, F.; He, X.; Hu, X. Resistance and durability of fly ash based geopolymer for heavy metal immobilization: Properties and mechanism. *RSC Adv.* **2024**, *14*, 12580–12592. [CrossRef] [PubMed]
14. Koike, Y.; Saito, R.; Kaseda, T.; Ohbuchi, A.; Ogawa, N. Elution Suppression Effect of Heavy Metals from Akadama Soil Mixed Municipal Solid Waste Fly Ash Geopolymer. *J. Soc. Inorg. Mater. Jpn.* **2024**, *31*, 33–38. [CrossRef]
15. Kaseda, T.; Hasuda, K.; Akino, Y.; Koike, Y.; Ogawa, N. Examination of a Water Washing Method for Radioactive Cesium in Municipal Solid Waste Incineration Fly Ash and a Separation-concentration Method for Washing Water. *Bunseki Kagaku* **2021**, *70*, 617–624. [CrossRef]
16. Takaoka, M.; Kawai, T.; Takeda, N.; Oshita, K. Recovery of heavy metals in fly ash from ash melting furnace by solvent extraction. *Environ. Eng. Res.* **2002**, *39*, 403–412. [CrossRef]
17. Sakanakura, H.; Kanno, K.; Matsuo, T.; Matsuto, T.; Tanaka, N. Factors Affecting the Stabilization of Heavy Metals in Air Pollution Control Residue from Municipal Solid Waste Incinerators Using Chelating Agents. *J. Jpn. Soc. Waste Manag. Expert.* **1999**, *10*, 187–195. [CrossRef]
18. Ogawa, N.; Amano, T.; Nagai, Y.; Hagiwara, K.; Honda, T.; Koike, Y. Water repellents for the leaching control of heavy metals in municipal solid waste incineration fly ash. *Waste Manag.* **2021**, *124*, 154–159. [CrossRef]
19. Koike, Y.; Kaseda, T.; Fukuda, T.; Ohbuchi, A.; Hagiwara, K.; Ogawa, N. Elution Suppression Treatment of Radioactive Cesium in Municipal Solid Waste Incineration Fly Ash Using Water-repellent Spray. *Jpn. J. Health Phys.* **2021**, *56*, 59–65. [CrossRef]
20. Ogawa, N.; Amano, T.; Koike, Y. Elution control of radioactive cesium in MSWI fly ash using water repellent treatment. *J. Mater. Cycles Waste Manag.* **2021**, *23*, 158–164. [CrossRef]
21. Akino, Y.; Tokumoto, Y.; Kaseda, T.; Hachiya, T.; Ogawa, N.; Koike, Y. Insolubilization of Heavy Metals in Municipal Solid Waste Incineration Fly Ash by Water Repellent Treatments using Fatty Acid. *J. Jpn. Soc. Mater. Cycles Waste Manag.* **2022**, *33*, 271–279. [CrossRef]
22. Rowthu, S.; Mattaparthi, S.; Siringil, E.; Hoffmann, P. Sewage Water-Repellent PDMS and Magnetic Silicone Composites: Lab to Commercialization. *ACS Appl. Polym. Mater.* **2023**, *5*, 6161–6175. [CrossRef]
23. Ministry of the Environment. Test Method of Metals Contained in Industrial Waste. 1973. Available online: https://www.env.go.jp/en/chemi/page_00001.html (accessed on 28 February 2023).
24. Zhang, J.; Seeger, S. Silica/Silicone Nanofilament Hybrid Coatings with Almost Perfect Superhydrophobicity. *Chemphyschem* **2013**, *14*, 1646–1651. [CrossRef]
25. Zhou, H.; Wang, H.; Niu, H.; Gestos, A.; Wang, X.; Lin, T. Fluoroalkyl Silane Modified Silicone Rubber/Nanoparticle Composite: A Super Durable, Robust Superhydrophobic Fabric Coating. *Adv. Mater.* **2012**, *24*, 2409–2412. [CrossRef]

26. Ke, W.-T.; Chiu, H.-L.; Liao, Y.-C. Multifunctionalized Cellulose Nanofiber for Water-Repellent and Wash-Sustainable Coatings on Fabrics. *Langmuir* **2020**, *36*, 8144–8151. [CrossRef] [PubMed]
27. Shibuichi, S.; Onda, T.; Satoh, N.; Tsujii, K. Super Water-Repellent Surfaces Resulting from Fractal Structure. *J. Phys. Chem.* **1996**, *100*, 19512–19517. [CrossRef]
28. Simpson, J.T.; Hunter, S.R.; Aytug, T. Superhydrophobic materials and coatings: A review. *Rep. Prog. Phys.* **2015**, *78*, 086501. [CrossRef] [PubMed]
29. Yang, G.; He, S.; Li, Y.; Li, Y.; Li, Z.; Song, W.; Chen, Z.; Liu, Q. Synthesis of reticular long-carbon-chain polysiloxane and its hydrophobic modification of phosphogypsum-based materials. *New J. Chem.* **2023**, *47*, 16713–16726. [CrossRef]
30. Perera, H.J.; Mortazavian, H.; Blum, F.D. Surface Properties of Silane-Treated Diatomaceous Earth Coatings: Effect of Alkyl Chain Length. *Langmuir* **2017**, *33*, 2799–2809. [CrossRef] [PubMed]
31. Young, R.P. Infrared spectroscopic studies of adsorption and catalysis. Part 3. Carboxylic acids and their derivatives adsorbed on silica. *Can. J. Chem.* **1969**, *47*, 2237–2247. [CrossRef]
32. Umemura, J.; Kamata, T.; Kawai, T.; Takenaka, T. Quantitative evaluation of molecular orientation in thin Langmuir-Blodgett films by FT-IR transmission and reflection-absorption spectroscopy. *J. Phys. Chem.* **1990**, *94*, 62–67. [CrossRef]
33. Ohbuchi, A.; Fujii, K.; Kasari, M.; Koike, Y. Characterization of soluble and insoluble radioactive cesium in municipal solid waste incineration fly ash. *Chemosphere* **2020**, *248*, 126007. [CrossRef]
34. Ohbuchi, A.; Fujii, K.; Koike, Y. Crystal Morphology Estimation of Trace Elements in MSWI Fly Ash Classified into Different Particle Sizes. *J. Jpn. Soc. Mater. Cycles Waste Manag.* **2019**, *30*, 144–152. [CrossRef]
35. Suzuki, K.; Kawamoto, K. Formation of Dioxins upon Heating Fly Ash from Municipal Solid Waste Incinerator during Thermal Treatment Process. *J. Environ. Chem.* **2004**, *14*, 239–251. [CrossRef]
36. Ministry of the Environment. Waste Disposal and Public Cleansing Law. 1973. Available online: https://www.env.go.jp/en/recycle/manage/sv.html (accessed on 27 November 2024).
37. Fujii, K.; Ochi, K.; Ohbuchi, A.; Koike, Y. Evaluation of physicochemical properties of radioactive cesium in municipal solid waste incineration fly ash by particle size classification and leaching tests. *J. Environ. Manag.* **2018**, *217*, 157–163. [CrossRef]
38. Gilardoni, S.; Fermo, P.; Gilanelle, V.; Pitea, D.; Collina, E.; Lasagni, M. MSWI Fly Ash Particle Analysis by Scanning Electron Microscopy-Energy Dispersive X-ray Spectroscopy. *Environ. Sci. Technol.* **2004**, *38*, 6669–6675. [CrossRef] [PubMed]
39. Takaoka, M.; Kuramoto, Y.; Takeda, N.; Fujiwara, T. Estimation of Spiecies of Zinc, Lead, Copper and Cadmium in Fly Ash by a Sequencial Chemical Extraction Method. *Doboku Gakkai Ronbunshu* **2001**, *8*, 79–90. [CrossRef]
40. Fukunaga, I.; Itoh, H.; Sawachi, M. Various Factors of Leaching for Detoxification Treatment of Fly Ash from Waste Incineration Plant. *Haikibutsugakkaishi* **1996**, *7*, 28–35. [CrossRef]
41. Yamaoka, S.; Morishita, T.; Ohtsubo, M.; Higashi, T.; Hagio, T. Leachability of heavy metals and soluble ions in the incineration ash by serial batch test. *Trans. Jpn. Soc. Irrig. Drain. Reclam. Eng.* **2006**, *246*, 41–47. [CrossRef]
42. Xiao, Y.; Huang, Y.; Cheng, H.; Zhu, Z.; Yu, M.; Xu, W.; Li, Z.; Zuo, W.; Zhou, H.; Jin, B. Advances and Outlook of Heavy Metal Treatment Technology from Municipal Solid Waste Incineration Fly Ash: A Review. *Energy Fuels* **2024**, *38*, 895–918. [CrossRef]
43. Osako, M.; Yamada, M.; Inoue, Y.; Kim, Y.-J.; Park, J.-K.; Lee, D.-H.; Yoshida, T.; Nomura, T. A Comparative Study on Leaching Characteristics of Heavy Metals from Municipal Solid Waste Incineration Bottom Ashes in Korea and Japan. *Haikibutsugakkaishi* **2001**, *12*, 256–265. [CrossRef]
44. Funatsuki, A.; Takaoka, M.; Kokubu, D.; Oshita, K.; Takeda, N. Speciation Analysis for Cadmium in Fly Ash. *Bunseki Kagaku* **2010**, *59*, 801–810. [CrossRef]
45. Kitamura, H.; Sawada, T.; Takahashi, F.; Shimaoka, T. Morphological surface conversions of municipal solid waste incineration fly ash after moistening. In Proceedings of the 24th Annual Conference of Japan Society Material Cycles and Waste Management, Tsukuba, Japan, 9–11 September 2024; Volume D7-14, pp. 623–624. [CrossRef]
46. Maeno, Y.; Hirata, T.; Nagase, H. Soil Mechanical Properties of Bottom Ash Obtained from Municipal Incinerators. *J. Jpn. Soc. Waste Manag. Expert.* **1998**, *9*, 29–38. [CrossRef]
47. Hiraoka, M.; Sakai, S. The properties of fly ash from municipal waste incineration and its future treatment technologies. *Haikibutsugakkaishi* **1996**, *7*, 28–35. [CrossRef]
48. Haynes, B.S.; Neville, M.; Quann, R.J.; Sarofim, A.F. Factors governing the surface enrichment of fly ash in volatile trace species. *J. Colloid Interface Sci.* **1982**, *87*, 266–278. [CrossRef]
49. Liu, P.; Feng, C.; Wang, F.; Gao, Y.; Yang, J.; Zhang, W.; Yang, L. Hydrophobic and water-resisting behavior of Portland cement incorporated by oleic acid modified fly ash. *Mater. Struct.* **2018**, *51*, 38. [CrossRef]
50. Harja, M.; Buema, G.; Bucur, D. Recent advances in removal of Congo Red dye by adsorption using an industrial waste. *Sci. Rep.* **2022**, *12*, 6087. [CrossRef]
51. Katara, S.; Kabra, S.; Sharma, A.; Hada, R.; Rani, A. Surface Modification of Fly Ash by Thermal Activation: A DR/FTIR Study. *Int. Res. J. Pure Appl. Chem.* **2013**, *3*, 299–307. [CrossRef]
52. Sekigawa, K.; Kobiyama, M. Adsorption of aliphatic carboxylic acids on aluminum surfaces. *Keikinzoku* **1991**, *41*, 304–310. [CrossRef]
53. Sakthivel, T.; Reid, D.L.; Goldstein, I.; Hench, L.; Seal, S. Hydrophobic High Surface Area Zeolites Derived from Fly Ash for Oil Spill Remediation. *Environ. Sci. Technol.* **2013**, *47*, 5843–5850. [CrossRef] [PubMed]

54. Zhao, J.; Wei, X.; Li, T.; Li, H.; Bin, F. Behavior of Alkali Metals in Fly Ash during Waste Heat Recovery for Municipal Solid Waste Incineration. *Energy Fuels* **2018**, *32*, 4417–4423. [CrossRef]
55. Omote, K. Structure analysis for organic thin filimsby grazing incidence X-ray diffraction. *Ouyoubutsuri* **2000**, *69*, 1441–1442. [CrossRef]